Journal of Microbiology (2017) Vol. 55, No. 4, pp. 280–288
DOI 10.1007/s12275-017-6320-z
eISSN 1976-3794
pISSN 1225-8873

Alteration in the ultrastructural morphology of mycelial hyphae and the dynamics of transcriptional activity of lytic enzyme genes during basidiomycete morphogenesis

Elena Vetchinkina[1]*, Maria Kupryashina[1], Vladimir Gorshkov[2,3], Marina Ageeva[2], Yuri Gogolev[2,3], and Valentina Nikitina[1]

[1]*Laboratory of Microbiology, Institute of Biochemistry and Physiology of Plants and Microorganisms, Russian Academy of Sciences IBPPM RAS, 13 Prospekt Entuziastov, Saratov 410049, Russian Federation*
[2]*Laboratory of Molecular Biology, Kazan Institute of Biochemistry and Biophysics, Kazan Science Center, Russian Academy of Sciences, 2/31 Lobachevsky street, Kazan 420111, Russian Federation*
[3]*Kazan Federal University, 18 Kremlyovskaya street, Kazan 420008, Russian Federation*

(Received Jul 5, 2016 / Revised Oct 28, 2016 / Accepted Nov 23, 2016)

The morphogenesis of macromycetes is a complex multilevel process resulting in a set of molecular-genetic, physiological-biochemical, and morphological-ultrastructural changes in the cells. When the xylotrophic basidiomycetes *Lentinus edodes*, *Grifola frondosa*, and *Ganoderma lucidum* were grown on wood waste as the substrate, the ultrastructural morphology of the mycelial hyphal cell walls differed considerably between mycelium and morphostructures. As the macromycetes passed from vegetative to generative development, the expression of the *tyr1*, *tyr2*, *chi1*, *chi2*, *exg1*, *exg2*, and *exg3* genes was activated. These genes encode enzymes such as tyrosinase, chitinase, and glucanase, which play essential roles in cell wall growth and morphogenesis.

***Keywords*:** basidiomycete morphogenesis, gene expression, lytic enzymes, phenol oxidases, cell wall ultrastructure

Introduction

The morphogenesis of basidiomycetes (alteration in their forms and developmental stages) is a multilevel dynamic process, taking place at both intracellular and intercellular levels throughout the fungal life cycle or under the influence of various environmental factors. This process implies molecular-genetic, physiological, and ultrastructural transformations and cell differentiation. Macromycetes differ substantially from all other microorganisms in terms of specific features of their morphogenesis. There is still a lack of information on the molecular and physiological aspects of the morphogenetic development in the basidiomycetes.

The key role in macromycete morphogenesis is played by the cell wall – a complex, biochemically and morphologically dynamic structure. Changes in its composition trigger cell differentiation, serving a specific functional purpose: vegetative growth, space colonization, ability to protect the organism from adverse environmental conditions and pathogens, and ability to form morphostructures and basidia (Bartnicki-Garcia, 1973; Michalenko *et al.*, 1976; Feofilova, 1983; Cabib *et al.*, 1988; Bowman and Free, 2006). The basidiomycete cell wall contains a large amount of chitin, which forms complexes with β-glucans. The glucans, along with chitins, are the predominant polysaccharides of this structure. They are responsible for the shape and rigidity of the mycelial hyphae (Cabib *et al.*, 1988; Fontaine *et al.*, 1997; Feofilova, 2002). Research on the biosynthesis of basidiomycete cell wall components demonstrates that chitins, glucans, and glycoproteins are covalently cross-linked and that the formation of this linkage is a dynamic process (Bowman and Free, 2006). The growth pattern of the cell wall and its transformation during morphogenesis involves a certain role of lytic enzymes in maintaining the balance between synthesis and lysis of its components (Bartnicki-Garcia, 1973; Kamada *et al.*, 1985; Herrera-Estrella and Chet, 1999).

The aim of this study was to examine the relationship between the ultrastructural morphology and differentiation of the mycelial hyphae of the basidiomycetes (nonpigmented mycelium, mycelial mat, primordia, and fruiting bodies) during morphogenesis, alongside the dynamics of the transcriptional activity of the enzyme genes (*tyr1*, *tyr2*, *chi1*, *chi2*, *exg1*, *exg2*, and *exg3*) which code for tyrosinase, chitinase, and glucanase, enzymes involved in the rearrangement of the basidiomycete cell wall.

Materials and Methods

Fungal strains and cultivation conditions

We used three types of medicinal cultivated xylotrophic basidiomycetes of different systematic groups. *Lentinus edodes* (Berk.) Sing F-249 (shiitake mushroom), *Grifola frondosa* (Fr.) S.F. Gray 0917 (maitake mushroom), and *Ganoderma lucidum* (Curtis: Fr.) P. Karst) 1315 (reishi or lingzhi mushroom) were obtained from the Collection of Higher Basidial Fungi, Department of Mycology and Algology, Lomonosov Moscow State University, and from the Basidiomycete Culture Collection of the Komarov Botanical Institute, Russian Academy of Sciences (RAS). The fungi were maintained in

*For correspondence. E-mail: elenavetrus@yandex.ru; Tel.: +78452970403; Fax: +78452970383

the collection of higher fungi held by the Laboratory of Microbiology at the IBPPM RAS on beer-wort (4 degrees on the Balling scale for sugar content) (Ball, 2006) and on 2% agar plates at 4°C. The basidiomycetes were grown by an intensive technique under conditions closest to natural. Growth through all stages of development was on a wood substrate under laboratory conditions. The morphogenesis of the basidiomycetes under study includes the following stages: active development of a substratum, growth and branching of nonpigmented mycelium (NM); consolidation of the mycelium on the substratum surface, pigmentation; formation of a protective morphological structure – a mycelial mat (MM) and formation of generative basidia – primordia (PR) and fruiting bodies (FB) (Vetchinkina and Nikitina, 2007).

Isolation of RNA and synthesis of cDNA by reverse transcription

Tissues of the morphostructures (nonpigmented mycelium, mycelial mat, primordia, and fruiting bodies) of *L. edodes*, *G. frondosa*, and *G. lucidum* were separately collected, immediately frozen, and homogenized by grinding in a porcelain mortar with liquid nitrogen. Total RNA was isolated from fungal cells by using an RNeasy Plant Mini kit (Qiagen) according to the manufacturer's recommendations. The RNA concentration was determined on a NanoDrop ND-1000 spectrophotometer (NanoDrop Technologies). The quality of the isolated RNA was assessed by electrophoretic separation patterns in 1% agarose gel after staining with ethidium bromide (Osterman, 1981).

For cDNA, we used 1.5 μg of total RNA pretreated with 0.1 U/μl DNase (Fermentas) at 37°C for 30 min. Reverse transcription was performed in a reaction mixture of the total volume of 25 μl containing 100 μM oligo-dT18 primers, 300 μM dNTPs, and 100 U M-MuLV reverse transcriptase (Fermentas) in a relevant buffer. First, an RNA solution was heated at 70°C for 5 min in the presence of oligonucleotide primers (oligo-dT18) and then cooled on ice. Then, the remaining components were added and the mixture was incubated at 37°C in a DNA Engine thermocycler (Bio-Rad) for 60 min. The reaction was terminated by heating the mixture to 70°C for 10 min. Two microliter of the cDNA thus obtained was used in PCR.

Amplification of DNA fragments by real-time PCR (qPCR)

To amplify *L. edodes*, *G. frondosa*, and *G. lucidum* DNA fragments (cDNA), we constructed primers complementary to fragments of the genes *tyr1*, *tyr2*, *chi1*, *chi2*, *exg1*, *exg2*, *exg3*, *gpd1*, and *gpd2*, which encode tyrosinase, chitinase, glucanase, and glyceraldehyde 3-phosphate dehydrogenase, respectively. The *gpd1* and *gpd2* genes were used for reference.

Primers were constructed by using the Vector NTI version 9 software package with the nucleotide sequences of *L. edodes* (Sakamoto *et al*., 2005a, 2005b, 2009). Since the information on the shiitake, maitake and reishi genome sequences in available databases is very limited, we compensated for the lack of data by building consensus sequences of the coding regions of the genes by using the existing databases on other basidiomycete species. The primers were synthesized by Syntol (Table 1).

PCR was done in a reaction mixture (total volume of 25 μl) that contained buffer [67 mM Tris-HCl; pH 8.8, 17 mM $(NH_4)_2SO_4$, 2.5 mM $MgCl_2$, and 0.1% Tween 20], 100 μM of each dNTP, 2 μl of cDNA, 0.1 μM of each primer. The temperature and duration of the reaction stages (10 sec at 94°C and 1 min at 60°C) were controlled with a CFX96 thermal cycler (Bio-Rad) equipped with an optical module. The duration of the procedure was 40 cycles.

The content of cDNA, corresponding to transcripts of each of the genes under study, was determined with calibration curves built on the basis of the reactions performed with four tenfold dilutions of cDNA. To evaluate the efficiency of the reactions and to build the calibration curves, we used the CFX Manager Software package (Bio-Rad). The absence of considerable amounts of genomic DNA was confirmed by PCR with the samples omitted from the reverse transcription. The relative level of expression was determined by comparing the amount of cDNA in a target gene (*tyr1*, *tyr2*, *chi1*, *chi2*, *exg1*, *exg2*, or *exg3*) with that in a reference gene (*gpd1* or *gpd2*).

Sample preparation for transmission electron microscopy

For studying the macromycete cell structure during morphogenesis, the cultures were investigated by transmission electron microscopy (TEM). The mycelial hyphae at different stages of morphogenesis were fixed with a 2.5% glutaraldehyde solution in phosphate buffer (0.1 M, pH 7.2) for 2 h and were postfixed with a 1% OsO_4 solution for 3 h in the same buffer containing sucrose (25 mg/ml). The samples were dehydrated in a series of alcohol solutions of increasing concentrations and in absolute acetone. Then, the samples were transferred into propylene oxide for 45 min, mixtures of Epon resin (Fluka) and propylene oxide at 1 : 2, 1 : 1, and 2 : 1 ratios (24 h each), and pure resin. The resin was polymerized at 37, 45, and 57°C (24 h each).

Sections were prepared on an LKB-III (LKB) microtome. Semithin cross-sections (2 μm) were stained with 1% meth-

Table 1. The list of the constructed primers

Primers	5′→3′ sequence
*gpd*1 F	GACGCACTGACAATCTGACTG
*gpd*1 R	GATGCGAGAGTTCAGGTTTTAC
gpd2 F	GAAGGGTGGTGCCAAGAAGGTG
gpd2 R	GCAGACGAACATGGGAGCATC
tyr1 F	GCCCAGGTTGATCGTCTGCTTTC
tyr1 R	CTGCCAATGTGACCGATACGTCC
tyr2 F	CAACCCTTCTGGGACTGGGC
tyr2 R	CGGTAGCGACGGAGTGGATT
chi1 F	CTTCGGGAGCCTATGTAACTGTG
chi1 R	CCAGGCTTTCCAATGATTACTGC
chi2 F	GACGTGAACAAGCTGGTCATCG
chi2 R	GGGAACTGGAACGCCATGAC
exg1 F	CGGGGTAAGTTCTCCTCCAAG
exg1 R	GAACGAGTAGGACGAACCATG
exg2 F	GTCAACCAAAACAACTTCTTCCGC
exg2 R	GAGACCTGCCAGTGGATACCG
exg3 F	CCAGCAGTTCACGGTCCG
exg3 R	GAAGGTCCAGCCCCAGTTCC

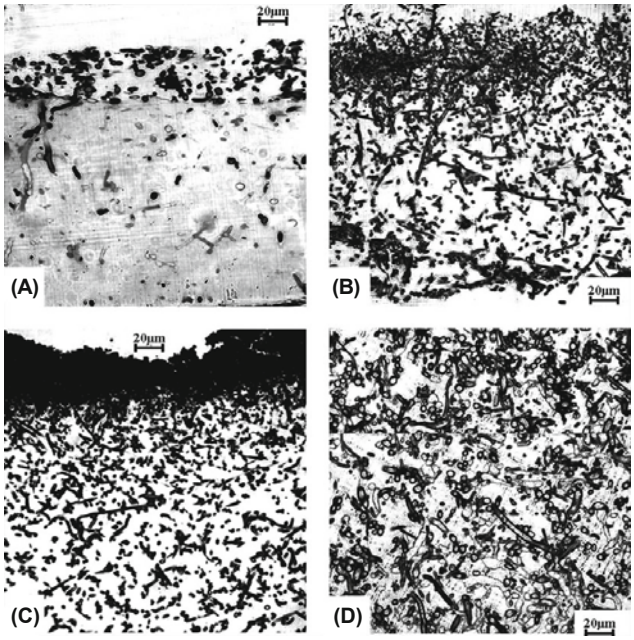

Fig. 1. Light microscopy of semithin sections of *L. edodes* mycelial hyphae at various morphogenesis stages. (A) friable nonpigmented mycelium, (B) tight nonpigmented mycelium, (C) mycelial mat, (D) primordia. Scale bar is 20 μm.

ylene blue for 30 sec and examined with a Leica DM6000B microscope (Leica Microsystems). Ultrathin sections were placed on nickel grids and stained with 2% aqueous uranyl acetate and Reynold's lead citrate solution (Reynolds, 1963). The ultrastructure of fungal cells at various stages of morphogenesis was analyzed on a JEM-1200 EX (JEOL) transmission electron microscope at an accelerating voltage of 80 kV.

Statistical analysis

The experiments were done in three replicates of three independent experiments. The data were processed by standard mathematical approaches (mean square root deviation calculation and comparison of the means by Student's *t*-test), by using Microsoft Excel 2000 software.

Results

Specific features of mycelial growth and the cell structure, depending on the fungal development stage

A light microscopy study of semithin cross-sections of nonpigmented rough mycelium indicated that the hyphae (3–4 μm in diameter) formed a 40–50 μm layer over the substrate. The hyphae penetrating into the substrate are much less densely located than the outer ones (Fig. 1A).

The cross-sections of the nonpigmented thick mycelium demonstrated its heterogeneity. In the top section, hyphae were more densely packed; there were many thin ones among them (approx. 1 μm in diameter). The diameter of the hyphae in the lower section, immediately adjacent to the substrate, was 2–3 μm. In addition, the hyphae were embedded in the intercellular matrix (Fig. 1B).

On the mycelial mat surface, the hyphae had a diameter of 2.5 μm and were very tight against each other, forming a 40–50-micron-thick highly pigmented protective layer. The protoplast remained intact; only the outermost cell layer appeared to be dead. The outer matrix was denser than that in primordia (Fig. 1C). Primordial hyphae were embedded in the intercellular matrix of rough fibrillar structure and had the largest diameter (4–5 μm) (Fig. 1D).

Transmission electron microscopy of the cell structure at different morphogenesis stages

In microphotographs of ultrathin sections, septated hyphae were observed. Dolipores and parentosomes with multiple holes were also seen clearly. In addition to the septa a large number of individual channels, responsible for cytoplasmic material transportation during mitosis (Suh *et al.*, 1993; Jenkinson *et al.*, 2008), were observed (Fig. 2A and B).

The cells were rich in cytoplasm and had one or several small vacuoles, transparent or with fibrillar contents. The chondriome was well-developed; the mitochondria were branchy and orthodox-type, stretching along the hyphae (Matrosova

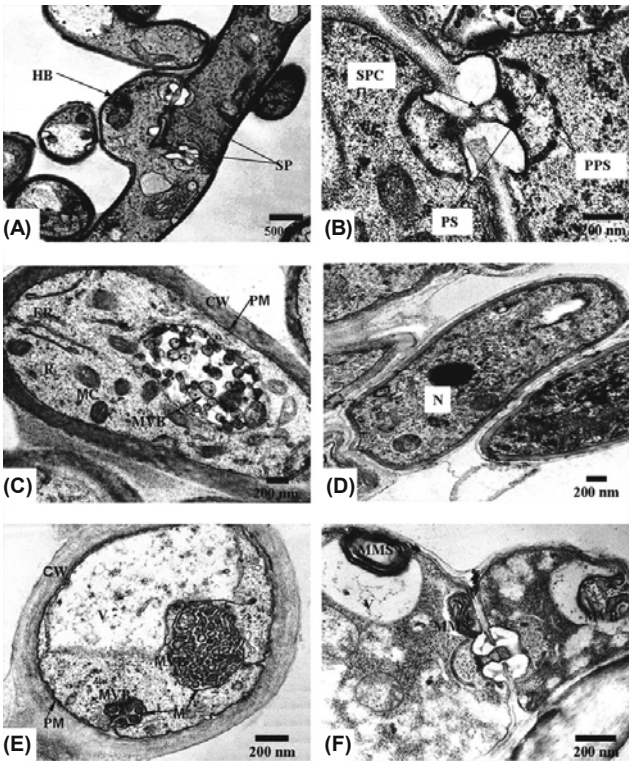

Fig. 2. Transmission electron microscopy (TEM) of longitudinal and transverse cross-sections of the mycelial hyphae of *L. edodes* (A, C, E), *G. frondosa* (B, D), and *G. lucidum* (F). Ultrastructure of the nonpigmented mycelial cells: hyphal buckle (HB), septum (SP), septal pore cap (SPC), parentosome (PS), pore of the parentosome (PPS), cell wall (CW), plasma membrane (PM), mitochondria (MC), ribosomes (R), endoplasmic reticulum (ER), nucleus (N), multivesicular bodies (MVB), vacuoles (V), multimembrane structures (MMS). Scale bar is 200 and 500 nm.

et al., 2009). The cytoplasm contained many free ribosomes. The endoplasmic reticulum was mostly smooth and well-developed; some of its cisterns were extra-wide. The vacuolar system was well-developed. There were numerous secretory vesicles, which were morphologically heterogeneous and had transparent or gray homogenous contents; the membrane was thin (Fig. 2C). The nuclei, surrounded by a two-layer membrane, both in the nonpigmented mycelial hyphae and in the cells at different developmental stages, had an orthodox structure and, as a rule, a round or oval shape (Fig. 2D). Multivesicular bodies were present in all the cells as an aggregation of vesicles (either surrounded by a membrane or, rarely, not). Because their membrane was similar to the plasmalemma, we assume that they were, in fact, endosomes formed through endocytosis, and they contained material obtained from outer areas (Fig. 2E). The multivesicular bodies were able to invaginate a vacuole, and, as a result of this, membrane "bundles" (myelinlike structures) were formed (Fig. 2F) (Kamzolkina *et al*., 2014).

The cell ultrastructure, in general, was only slightly different, depending on the location of the cells. The mitochondria formed large groups, and there were many polysomes. The vacuoles varied in size and had fibrillar contents. The edge cells were more vacuolated and contained some multivesicular bodies. The lower-section hyphae were characterized by intensive secretion; there were many secretory vesicles, and their association with the plasmalemma was clearly observed. Spherical lipid drops and a large amount of glycogen were also seen.

Unlike cells at the nonpigmented mycelium stage, cells at the mycelial mat stage had a thickened cell wall (an electron-dense layer consisting of chitin fibrils embedded in a β-glucan matrix) (Fig. 3A). Also characteristic were a large number of vacuoles, some of which were autolytic. The vacuoles often contained granular polyphosphate inclusions (Fig. 3A and B). These cells contained fewer ribosomes and less rough endoplasmic reticulum, as compared to the cells at the other stages. Various multivesicular and myelinlike structures were present in great abundance (Fig. 3B and C).

Primordial hyphae, as mentioned above, were embedded in the intercellular matrix of rough fibrillar structure. They had the largest diameter among the cells under study – 4 to 5 μm. The cell wall was thickened (1 μm) and had a characteristic "speckled" texture (although thin-walled hyphae were also observed). In cells with a thickened cell wall, condensation of the cytoplasm was observed, while the lumen in the cross-section was star-shaped (Fig. 3D). These hyphae, in all likelihood, perform a supporting function. The cells were heterogeneous and differed in the degree of their vacuolation and in the density of their cytoplasm. The hyphae had vacuoles of different sizes with fibrillar contents, sometimes with small osmiophilic spheres (Fig. 3E). Occasionally, large vacuoles were formed (sometimes 80 nm in diameter), as were vesicles, which were pressed against one another and had dense dark inclusions – polyphosphate granules (Fig. 3F). The mitochondria were orthodox-type. The endoplasmic reticulum was generally rough (unlike the nonpigmented mycelium). However, smooth reticulum and numerous polysomes were also observed. Microtubules could also be clearly seen. Unlike the mycelia at the other stages of development, the secretory vesicles were not numerous, and there were no fringed vesicles (Fig. 3F).

In fruiting bodies, the vacuolar system was well-developed. Most of the cells had several vacuoles, which were pressed against each other and occupied most of the cellular space (Fig. 3G). We detected spherical lipid drops and granular polyphosphate inclusions. Some of the cells were filled with glycogen (they performed the role of depositories of this product) (Fig. 3H).

We also observed "supporting" hyphae with a thickened cell wall, as well as greatly pigmented cells (Fig. 3I). We assume that in fruiting bodies, the functional differentiation of cells or specific cell segments is well-developed.

Transmission electron microscopy of the ultrastructure of mycelial cell walls at different morphogenesis stages

The ultrastructural morphology of the mycelial cell wall and

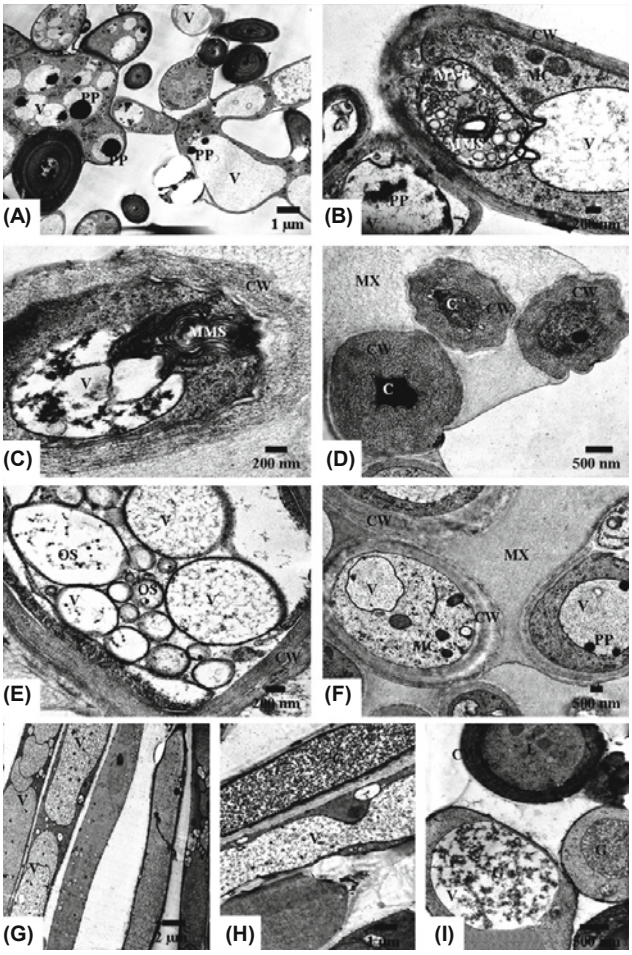

Fig. 3. Transmission electron microscopy (TEM) of longitudinal and transverse cross-sections of the mycelial hyphae of *L. edodes*, *G. frondosa*, and *G. lucidum*. Ultrastructure of the mycelial hyphae at various morphogenesis stages: (A, B, C) mycelial mat, (D, E, F) primordia, (G, H) fruiting body (stipe), (I) fruiting body (cap). Cell wall (CW), vacuoles (V), polyphosphate (PP), mitochondria (MC), multivesicular bodies (MVB), multimembrane structures (MMS), extracellular matrix (MX), cytoplasm (C), osmiophilic pellets (OS), lipid droplet (L), glycogen (G). Scale bar is 200; 500 nm and 1; 2 μm.

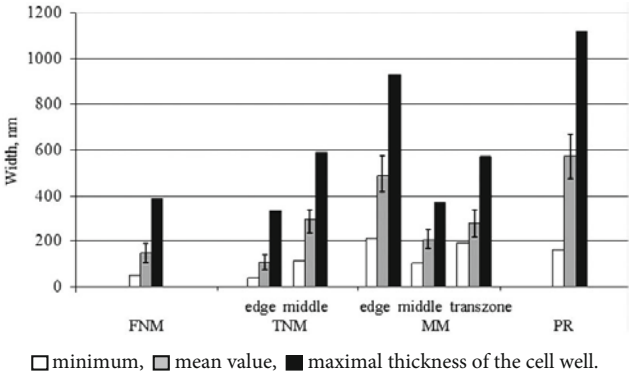

Fig. 4. Thickness of the cell wall mycelial hyphae of *L. edodes* at different stages of morphogenesis. The arrangement of cells in a tissue: edge (the outside edge), middle, transzone (adjacent to the substrate); (FNM) friable nonpigmented mycelium, (TNM) tight nonpigmented mycelium, (MM) mycelial mat, (PR) primordia.

morphostructures varied, depending on the macromycete's stage of development. The rough nonpigmented mycelial cell wall was approximately 150 nm thick. Although the hyphae penetrating the substrate were much less densely packed (as compared to the cell layer on the surface), their diameter, as well as the cell wall thickness, remained the same. As the basidiomycetes underwent further development and the density of the nonpigmented mycelium increased, both differentiation of the mycelial hyphae and alteration of the cell wall ultrastructure took place.

On the outer side, the hyphae became denser and shrank substantially. Many thin hyphae (1 μm in diameter) could be seen, and their cell walls were approximately 100 nm thick. At the stage of dense nonpigmented mycelium, the hyphae immediately adjacent to the substrate and embedded in the matrix had cell walls whose size increased, ranging from approx. 300 to 600 nm in some instances (Fig. 4).

The microphotographs clearly show the cytoplasmic membrane and the two-layer cell wall adjacent to it. This cell wall consists of an inner electron-dense layer of fibrillar structure (chitin fibrils embedded in a β-glucan matrix) and an outer electron-transparent layer containing an alkali-soluble glucan (Fig. 5A and B).

The pigmented mycelial mat showed an even greater cytodifferentiation of mycelial hyphae. The cell wall ultrastructure differed substantially, depending on the cells' location (Fig. 5C). Unlike the thin-walled hyphae at the preceding development stage, the outer layer of the cell wall was substantially thickened (from 450 to 950 nm). Besides, the hyphae were highly melanized and very closely adjacent to one another, forming a tight frame (approx. 50 μm thick) (Fig. 5D and E).

During the thickening of the mycelium, there appeared many pigmented thick-walled hyphae in the macromycetes (*G. lucidum* had a considerably greater number of those than did *L. edodes* or *G. frondosa*; besides, the cell wall of the latter fungi was less thick) (Fig. 5C–E). The cell layer located in the middle section of the tissue was less dense; the cell wall was approximately 200 nm thick. The density of the cells closely adjacent to the substrate, as well as their cell wall thickness, corresponded to the values obtained at the preceding developmental stage (dense nonpigmented mycelium), ranging from 280 to 570 nm (Fig. 5B).

At the primordial stage, the fungal cell walls had the greatest thickness (approx. from 600 nm to 2 μm in some instances) and a characteristic "speckled" texture. However, thin-walled hyphae were also present (Fig. 5F). In thick-walled cells, the cytoplasm got denser, and the lumen acquired the shape of a star (Fig. 5G). These hyphae apparently fulfill a supporting function. At this particular stage, unlike the ones described above, the "supporting" hyphae were especially numerous, and owing to this, the macromycetes were able to maintain the shape of the basidiomes formed. The fruiting bodies often had "supporting" hyphae with ultrathick pigmented cell walls (Fig. 5H).

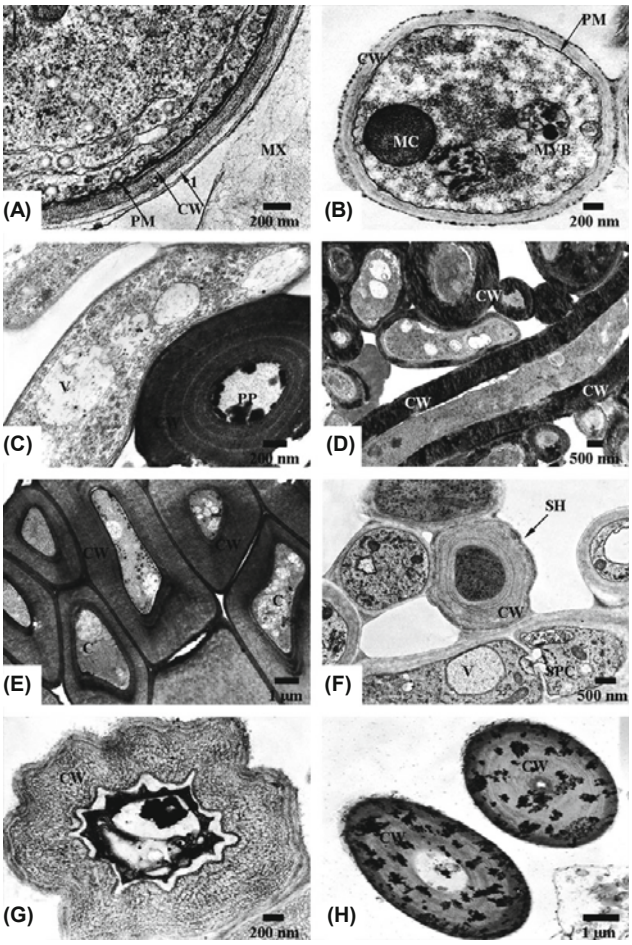

Fig. 5. Ultrastructural alterations (TEM) in the basidiomycete cell wells at different stages of morphogenesis. A thin-walled cell of the nonpigmented mycelium of *L. edodes* (A); a cell of the pigmented mycelium of *G. frondosa* with a thickened cell wall (B); a supporting hypha of the mycelial mat of *G. lucidum* with an ultrathick melanized cell wall (C); highly melanized thickened cell walls of the mycelial mat of *L. edodes* (D); pressed, heavily pigmented thick-walled hyphae of the mycelial mat of *G. lucidum* (E); a thick-walled supporting hypha of the *L. edodes* primordia (F); a star-shaped primordial cell of *L. edodes* (G); thick-walled melanized cells of the fruiting body (stipe) of *L. edodes* (H). Cell well (CW): 1, external electron-transparent layer, 2, internal electron-dense layer; supporting hyphae (SH); for other designations, see Figs. 2 and 3. Scale bar is 200; 500 nm and 1 μm.

Dynamics of expression of tyrosinase, chitinase, and glucanase genes (*tyr1*, *tyr2*, *chi1*, *chi2*, *exg1*, *exg2*, and *exg3*), depending on the developmental stage

Transcripts of the genes under study (*tyr1*, *tyr2*, *chi1*, *chi2*, *exg1*, *exg2*, and *exg3*) were detected at all stages of fungal morphogenesis. However, the level of their expression differed greatly, depending on the stage. Tyrosinase activity increased with increasing pigmentation intensity of the mycelium. PCR analysis showed that the highest level of *tyr1* and *tyr2* expression was at the stage of the mycelial mat – a

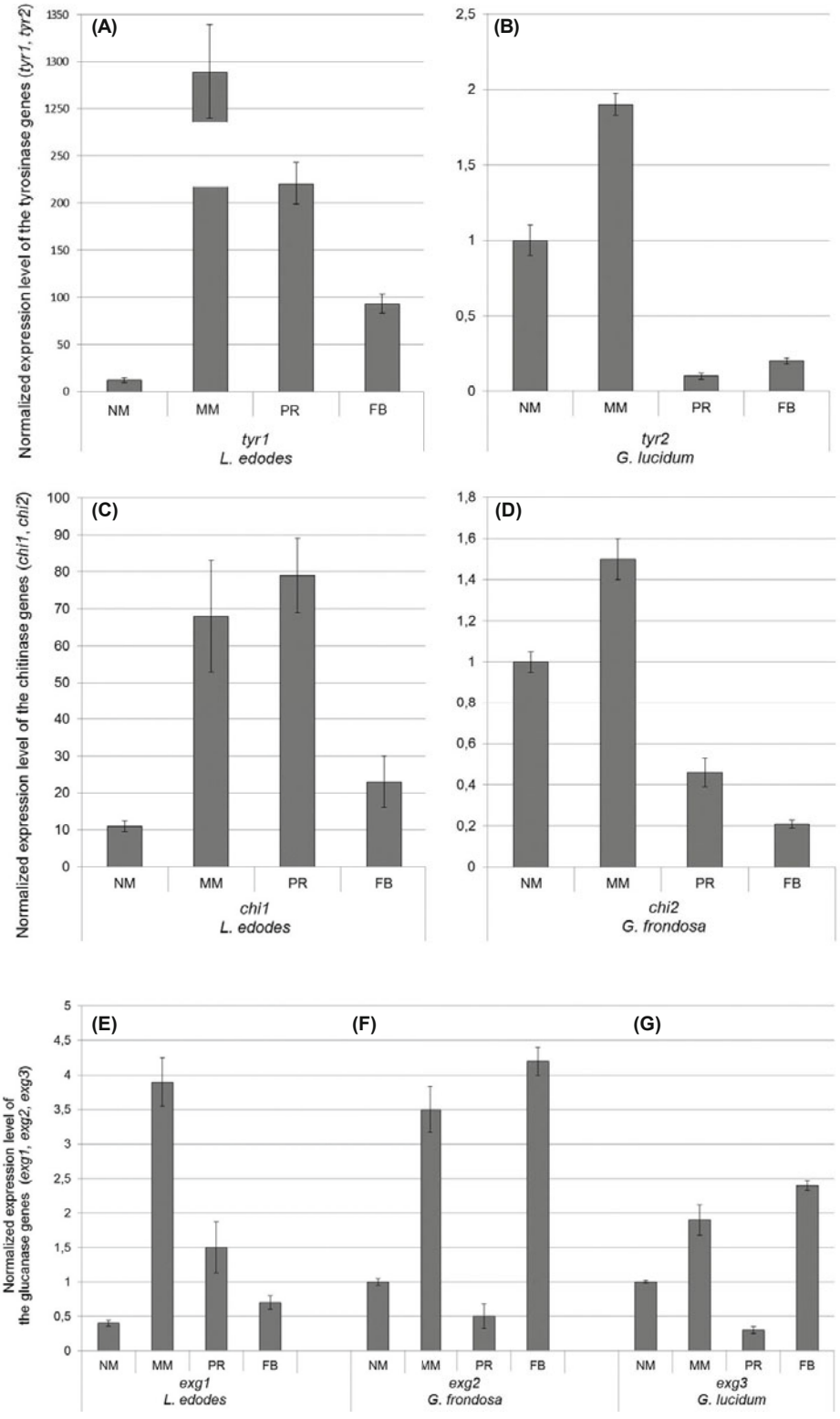

Fig. 6. Expression of the tyrosinase (A, B), chitinase (C, D), and glucanase (E, F, and G) genes in *L. edodes, G. frondosa,* and *G. lucidum* at various morphogenesis stages. The data are normalized by the transcriptional activity of the *gpd* gene. (NM) non-pigmented mycelium, (MM) mycelial mat, (PR) primordia, (FB) fruiting body.

highly melanized fungal structure (Fig. 6A and B).

According to the experimental data, the transition from vegetative growth to basidium formation was followed by a manifold increase in tyrosinase gene expression. All phenol oxidases, including tyrosinases, catalyze the synthesis of melanins, which perform a protective function. They are also responsible for fusing mycelial cell wall components during the formation of morphogenic structures (Thurston, 1994; Whitaker, 1995; Kanda *et al.*, 1996a, 1996b; Van Gelder *et al.*, 1997).

The level of the chitinase *chi1* and *chi2* gene expression was highest at the mycelial mat and primordium stages (Fig. 6C and D). The algorithm of fungal cell wall growth implies a specific role of lytic enzymes in maintaining the balance between cell wall synthesis and lysis (achieved through a cooperative effect of chitin syntase and chitinase activity) during the apical growth of the mycelium (Herrera-Estrella and Chet, 1999). Besides, a role for chitinase in hyphal division and branching was also proposed (Bartnicki-Garcia, 1973).

Most fungi synthesize glucanase enzymes, both extracellular and associated with the cell wall. According to our data, the basidiomycetes demonstrated the highest level of expression of the *exg1*, *exg2*, and *exg3* glucanase genes, as well as the *chi1* and *chi2* chitinase genes, at the mycelial mat, primordium (*L. edodes*), and fruiting body stages (*G. frondosa*, *G. lucidum*), unlike the nonpigmented vegetative mycelium (Fig. 6E, F, and G).

From our data, it is evident that intracellular glucanases and chitinases play a very important role in cellular rearrangements during vegetative mycelial growth, especially at the morphogenesis stages. Glucans, as well as chitin, are prevalent cell wall polysaccharides and have been assumed to be responsible for the shape and degree of rigidity of the hyphal wall (Cabib *et al.*, 1988; Fontaine *et al.*, 1997).

Discussion

Analysis of the electron microscopy data shows that during fungal growth, substrate colonization, and alterations in the morphogenesis stages, the fungal hyphae undergo substantial changes, and intracellular ultrastructural rearrangements, along with the cytodifferentiation in the mycelium, take place. Especially notable are the transformations of the cell wall structure, one of the most important systems determining the direction of the basidiomycetes' morphogenetic development (Gull and Newsam, 1975; Saksena *et al.*, 1976). *L. edodes*, *G. frondosa*, and *G. lucidum* are xylotrophs making use of wood as a food substrate. At their initial development stages, following inoculation, the nonpigmented mycelial hyphae demonstrate active growth, division, and substrate colonization. At this stage, all the cell diameters, as well as their wall thickness, remain the same. Further on, mycelial hyphal differentiation takes place. Along with that, a dense mycelial layer is formed on the substrate's surface, and its hyphae are embedded in the matrix. In addition, the cell walls thicken two- to four-fold. Later on, the nonpigmented mycelium gets even denser and becomes pigmented; a layer of tightly intertwined thick-walled melanized hyphae covers the white mycelium, and a mycelial mat is formed. At this stage, further cytodifferentiation takes place, and the cell wall ultrastructure becomes substantially different, depending on the cells' location. The layers of the cells located in the middle section of the tissue and those closely adjacent to the substrate are similar to the layers at the preceding development stage in terms of their wall density and thickness. The outer mycelial cells thicken considerably (up to 1 μm) and are closely adjacent to one another; intercellular adhesion is also enhanced, owing to which a multicellular structure is formed that protects the organism from adverse environmental conditions. The formation of a mycelial mat is typical of all the basidiomycetes studied in this work; however, it varies in terms of its density, cell wall thickness, and pigmentation intensity (beige in *G. frondosa,* red in *G. lucidum*, and dark-brown in *L. edodes*). Apparently, during evolution, this structure emerged as an adaptive mechanism protecting both the nonpigmented mycelium and the forming primordia from adverse environmental conditions. The formation of the mat precedes fruiting; beneath its surface, primordia are formed [their cell walls are the thickest (up to 2 μm), compared to those formed at the other morphogenesis stages described above]. There emerge many "supporting" hyphae, which are responsible for the morphology of the macromycetes' reproductive organs. Thus, the ultrastructural morphology of the hyphal cell walls varies strongly, depending on the morphogenesis stage.

The basidiomycete cell walls contain a large amount of chitin, which forms complexes with β-glucans (Feofilova, 1983, 2002; Mendoza, 1992). For instance, in basidiomes of *Agaricus* fungi, chitin fibrils embedded in a β-glucan matrix make up more than 80% of the cell wall (Michalenko *et al.*, 1976). It is evident that since chitins and β-glucans, which form complexes, are the prevalent polysaccharides of the cell wall and define its shape and degree of rigidity (Cabib *et al.*, 1988; Fontaine *et al.*, 1997), lytic enzymes must play an important role in the growth and morphogenesis of the fungal cell wall, which is to maintain the balance between the synthesis and lysis of its components. For example, endo-β-glucanase enzymes are involved in the constant rearrangement of the cell wall's glucans during mycelial growth (Polacheck and Rosenberger, 1975), and they play an important role in stretching the stipe fibers of the basidiomycete *Coprinus cinereus* (Kamada *et al.*, 1985).

The expression of the *exg1*, *exg2*, *exg3*, *chi1*, and *chi2* genes reached the top level at the mycelial mat, primordium, and fruiting body stages, at which the cell walls thickened and stretched considerably in contrast to the thin-walled hyphae of the nonpigmented mycelium. In addition, a large number of thick-walled "supporting" hyphae emerged. The basidiomes and dense mycelial structures (mats, sclerotia) contained much more chitin and glucan than the nonpigmented vegetative mycelium submerged into the substrate (Kozlova and Kamzolkina, 2004). Our data show that at these developmental stages, the transcriptional activity of the *exg* and *chi* genes increased, triggering the corresponding amplification of synthesis of chitinases and glucanases – intercellular enzymes that are essential for cell wall morphogenesis. Besides, this evidence suggests that both chitinase and glucanase are involved in the incessant rearrangement of the cell wall polysaccharides. They have an immediate effect on

this structure's polymers (β-1,3-glucans, bound to chitin, another essential component) and can make the fungal cell wall more rigid or flexible during the apical growth, branching, consolidation, stretching, or fusion of the fungal hyphae, responsible for the formation of macromycete morphostructures. Study of the biosynthesis of the different components of the fungal cell wall proves that chitins, glucans, and glycoproteins are covalently cross-linked and that the formation of this linkage is a dynamic process (Bowman and Free, 2006).

Besides, phenol oxidases such as tyrosinases, employed by xylotrophic basidiomycetes for degrading wood and supplying themselves with nutrients, may also participate in fungal cell wall morphogenesis (Raguz *et al*., 1992; Perry *et al*., 1993; Thurston, 1994; Kanda *et al*., 1996a, 1996b; Van Gelder *et al*., 1997). According to our evidence, the expression of the tyrosinase *tyr1* and *tyr2* genes was highest at the most strongly pigmented developmental stage – the mycelial mat. This is quite understandable, as tyrosinase is involved in the synthesis of melanin, which makes fungi tolerant of environmental conditions. Dense structures, fulfilling a protective function at the onset of fruiting body formation, are heavily saturated with pigments. It is believed that melanin provides resistance to ultraviolet light. Besides, this pigment has a substantial effect on the resistance of the chitin-glucan-melanin complex to chitinase and 1,3-β-glucanase action (Feofilova, 1983; Whitaker, 1995). The pigments cluster either on the hyphae's outer surface (in granulated form) or inside the fungal cell wall, forming a complex with chitin. This results in the formation of a strong pathogen-resistant barrier.

Our data indicate a multifaceted role for tyrosinases, chitinases, and glucanases in the development of xylotrophic basidiomycetes. They suggest that these enzymes contribute not only to substrate colonization but also to shifts in the morphogenesis stages, as well as to the ultrastructural rearrangement of the fungal cell wall components. This indicates that these compounds and/or their products have regulatory activity during macromycete development.

Conclusions

Thus, the manifold increase in the expression of the *exg1*, *exg2*, *exg3*, *chi1*, *chi2*, *tyr1*, and *tyr2* genes with cytodifferentiation at different development stages suggests that intracellular glucanases, chitinases, and tyrosinases play a key role in the tightening, stretching, pigmentation, and binding of the cell wall components and in the fusion of hyphae, all these processes being essential for the formation of morphostructures in macromycetes. The maximal enzymatic activity at the pigmented mycelial mat stage suggests an important role of this structure in morphogenesis. The mycelial mat not only fulfills a protective function but, being biochemically active, also facilitates fruiting body formation. The ultrastructural rearrangements of the hyphal cell wall, taking place at the transition from one developmental stage to the next, along with the changing dynamics of the transcriptional activity of the key genes during morphogenetic development, confirms the status of the cell well as one of the most important systems responsible for the direction of the morphogenesis of basidiomycetes, fungi that are of great interest owing to their nutritive value and unique medicinal properties.

Acknowledgements

This study was supported by the Russian Foundation for Basic Research (project no. 15-04-02926).

References

Ball, D.W. 2006. Concentration scales for sugar solutions. *J. Chem. Educ.* **83,** 1489–1491.

Bartnicki-Garcia, S. 1973. Fundamental aspects of hyphal morphogenesis. *Symp. Soc. Gen. Microbiol.* **23**, 245–257.

Bowman, S.M. and Free, S.J. 2006. The structure and synthesis of the fungal cell wall. *Bioassays* **28**, 799–808.

Cabib, E., Bowers, B., Sburlati, A., and Silverman, S.J. 1988. Fungal cell wall synthesis: the construction of a biological structure. *Microbiol. Sci.* **5**, 370–375.

Feofilova, E.P. 1983. Fungal Cell Wall. Nauka, Moscow, p. 248.

Feofilova, E.P. 2002. Key role of chitin in fungal cell wall, in Chitin and Chitosan: Production, Properties, and Application, pp. 91–111. Nauka, Moscow, Russia.

Fontaine, T., Hartland, R.P., Beauvais, A., Diaquin, M., and Latge, J.P. 1997. Purification and characterization of an endo-l,3-β-glucanase from *Aspergillus fumigatus*. *Eur. J. Biochem.* **243**, 315–321.

Gull, K. and Newsam, R.J. 1975. Meiosis in basidiomycetous Fungi I. Fine structure of spindle pole body organization. *Protoplasma* **83**, 247–257.

Herrera-Estrella, A. and Chet, I. 1999. Chitinases in biological control. *In* Jolles, P. and Muzarelli, R. (eds.), Chitin and chitinases, pp. 171–184. Birkhausen Verlag, Basel, Switzerland.

Jenkinson, T.S., Celio, G.J., Padamsee, M., Dentinger, B.T.M., Meyer, M.L., and McLaughlin, D.J. 2008. Conservation of cytoplasmic organization in the cystidia of *Suillus* species. *Mycologia* **100**, 539–547.

Kamada, T., Fujii, T., Nakagawa, T., and Takenaru, T. 1985. Changes in l,3-β-glucanase activities during stipe elongation in *Coprinus cinereus*. *Curr. Microbiol.* **12**, 251–260.

Kamzolkina, O.V., Mazheĭka, I.S., Shtaer, O.V., Kudriavtseva, O.A., and Mukhin, V.A. 2014. Endomembrane system of fungi: traditional and modern conceptions. *Tsitologiia* **56**, 549–561.

Kanda, K., Sato, T., Ishii, S., Enei, H., and Ejiri, S. 1996a. Purification and properties of tyrosinase isozymes from the gill of *Lentinus edodes* fruiting body. *Biosci. Biotechnol. Biochem.* **60**, 1273–1278.

Kanda, K., Sato, T., Suzuki, K., Ishi, S., Ejiri, S., and Enei, H. 1996b. Relationships between tyrosinase activity and gill browning during preservation of *Lentinus edodes* fruit-bodies. *Biosci. Biotechnol. Biochem.* **60**, 479–480.

Kozlova, M.V. and Kamzolkina, O.V. 2004. Ultrastructure of the cell wall in vegetative mycelia of *Agaricus bisporus*. *Tsitologiia* **46**, 191–201.

Matrosova, E.V., Mazheĭka, I.S., Kudriavtseva, O.A., and Kamzolkina, O.V. 2009. Morphogenesis and ultrastructure of basidiomycetes *Agaricus* and *Pleurotus* mitochondria. *Tsitologiia* **51**, 490–499.

Mendoza, C.G. 1992. Cell wall structure and protoplast reversion in basidiomycetes. *World J. Microbiol. Biotechnol.* **1**, 36–38.

Michalenko, G.O., Hohl, H.L., and Rast, D. 1976. Chemistry and architecture of the mycelial wall of *Agaricus bisporus*. *J. Gen. Microbiol.* **92**, 252–262.

Osterman, L.A. 1981. Methods for Investigation of Proteins and Nucleic Acids: Electrophoresis and Ultracentrifugation, p. 288. Nauka, Moscow, Russia.

Perry, C.R., Smith, M., Britnell, C.H., Wood, D.A., and Thurston, C.F. 1993. Identification of two laccase genes in the cultivated mushroom *Agaricus bisporus*. *J. Gen. Microbiol.* **139**, 1209–1218.

Polacheck, Y. and Rosenberger, R.F. 1975. Autolytic enzymes in hyphae of *Aspergillus nidulans*: their action on old and newly formed walls. *J. Bacteriol*. **121**, 332–337.

Raguz, S.I., Yagüe, E., Wood, D.A., and Thurston, C.F. 1992. Isolation and characterization of a cellulose-growth-specific gene from *Agaricus bisporus*. *Gene* **119**, 183–190.

Reynolds, E.S. 1963. The use of lead citrate at high pH as an electron opaque stain in electron microscopy. *J. Cell. Biol.* **17**, 208–212.

Sakamoto, Y., Irie, T., and Sato, T. 2005a. Isolation and characterization of a fruiting body-specific exo-beta-1, 3-glucanase-encoding gene, *exg1*, from *Lentinula edodes*. *Curr. Genet.* **47**, 244–252.

Sakamoto, Y., Minato, K., Nagai, M., Mizuno, M., and Sato, T. 2005b. Characterization of the *Lentinula edodes exg2* gene encoding a lentinan-degrading exo-beta-1, 3-glucanase. *Curr. Genet.* **48**, 195–203.

Sakamoto, Y., Nakade, K., and Sato, T. 2009. Characterization of the post-harvest changes in gene transcription in the gill of the *Lentinula edodes* fruiting body. *Curr. Genet*. **55**, 409–423.

Saksena, K.N., Marino, R., Haller, M.N., and Lemke, P.A. 1976. Study on development of *Agaricus bisporus* by fluorescent microscopy and scanning electron microscopy. *J. Bacteriol.* **126**, 417–428.

Suh, S.O., Hirata, A., Sugiyama, J., and Komagata, K. 1993. Septal ultrastructure of basidiomycetous yeasts and their taxonomic implications with observations on the ultrastructure of *Erythrobasidium hasegawianum* and *Sympodiomycopsis paphiopedili*. *Mycologia* **85**, 30–37.

Thurston, C.F. 1994. The structure and function fungal laccase. *J. Microbiol.* **140**, 19–26.

Van Gelder, C., Flurkey, W., and Wichers, H. 1997. Sequence and structural features of plant and fungal tyrosinases. *Phytochem.* **45**, 1309–1323.

Vetchinkina, E.P. and Nikitina, V.E. 2007. Morphological patterns of mycelial growth and fruition of some strains of an edible xylotrophic basidiomycete *Lentinus edodes*. *Izv. Samar. Nauch. Tsentr. Ross. Akad. Sci.* **9**, 1085–1090.

Whitaker, J.R. 1995. Food Enzymes: Structure and Function, p. 284. *In* Wong, D. (ed.), Chapman and Hall.